Wood Science and Technology (2024) 58:649–675
https://doi.org/10.1007/s00226-024-01533-6

ORIGINAL

Conservation of model degraded pine wood with selected organosilicons studied by XFM and nanoindentation

Magdalena Broda[1] · Joseph E. Jakes[2] · Luxi Li[3] · Olga A. Antipova[3] · Evan R. Maxey[3] · Qiaoling Jin[4]

Received: 24 August 2023 / Accepted: 15 January 2024 / Published online: 10 February 2024

Abstract

Previous research found that some organosilicon treatments proved effective in stabilizing waterlogged wood dimensions during drying. The present research aimed to determine the mechanism of wood stabilization by these chemicals to understand their mode of action. The study used chemically (ChP) and biologically degraded (BP) model Scots pine wood treated with Methyltrimethoxysilane (MTMS), (3-Mercaptopropyl) trimethoxysilane (MPTMS), or 1,3-Bis(diethylamino)-3-propoxypropanol)-1,1,3,3-tetramethyldisiloxane (DEAPTMDS). Synchrotron-based X-ray fluorescence microscopy (XFM) was used to investigate the penetration of organosilicons into the wood cellular structure and cell walls, and nanoindentation was used to study the mechanical properties of the treated wood cell walls. All treatments resulted in high volumetric anti-shrink efficiency (ASE_V) values of 74–82%, except for MTMS-treated ChP with an ASE_V of 52%. The multiscale XFM results revealed that all applied organosilicons penetrated throughout the whole wooden blocks and deposited in both cell lumina and cell walls. The retention of all applied organosilicons was highest in BP wood, and so was the dimensional stabilization effect. MTMS-treated ChP had the lowest measured cell wall infiltration, which likely contributed to its lower ASE_v. DEAPTMDS treatments plasticized the cell walls and resulted in lowered nanoindentation elastic modulus (E_s^{NI}) and hardness (H) for all types of wood. MTMS and MPTMS had modest effects on cell wall mechanical properties, and the effect depended on the type of wood. The final effect of organosilicon treatment on the dimensional wood stabilization and mechanical properties of wood cell walls depended not only on the type of the applied organosilicon but also the type of wood degradation. This means that the treatment cannot be considered universal, and specific approaches are needed for the conservation of individual wooden objects. Although some mechanisms are now better understood, such as the need for organosilicons to infiltrate the cell walls and the plasticizing

Magdalena Broda and Joseph E. Jakes have contributed equally to this work.

Extended author information available on the last page of the article

effect of DEAPTMDS, other aspects will benefit from a more detailed analysis of the molecular interactions between organosilicons and wood polymers.

Introduction

Organosilicon compounds like silanes and siloxanes are effective for surface protection and modification of commercial wood and wood-based products to decrease their hydrophilicity, enhance decay resistance, reduce flammability, and improve weathering performance (Tshabalala et al. 2003; Hill et al. 2004; Mai and Militz 2004; Donath et al. 2006; Panov and Terziev 2009; Giudice et al. 2013; Broda et al. 2018b; Yona et al. 2021). They can also improve dimensional wood stability (Hill et al. 2004; Mai and Militz 2004; Donath et al. 2004; Kumar et al. 2016; Schorr and Blanchet 2020). Therefore, we are studying them as potential consolidants for waterlogged archeological wood that requires dimensional stabilization during drying (Broda et al. 2019b, 2020).

Although some of the applied organosilicons successfully stabilized waterlogged wood dimensions, their effectiveness differed significantly depending on the wood species and the degree of wood degradation (Broda et al. 2019b, 2020). Therefore, the aim of the present research is to determine the mechanism of wood stabilization by organosilicon compounds to understand their mode of action and thus effectively apply them for the conservation of various wooden artifacts. The study was conducted on model degraded pine wood differing in the degree of degradation and chemical composition (Broda et al. 2022a, b) using three of the most effective organosilicon compounds: Methyltrimethoxysilane (MTMS), (3-Mercaptopropyl)trimethoxysilane (MPTMS), and 1,3-Bis-[(diethylamino)-3-propoxypropanol]-1,1,3,3-tetramethyldisiloxane (DEAPTMDS) (Broda et al. 2020; Broda and Yelle 2022; Broda and Plaza 2023). Model degraded wood was used because research on new conservation agents for waterlogged wood requires a lot of similarly degraded wood material, and natural historical waterlogged wood is usually not available in enough amount or varies significantly in the degree of degradation, as it has already been recognized by other researchers working on new wood conservation agents (Kennedy and Pennington 2014; Tahira et al. 2017; Liu et al. 2019). Synchrotron-based large-field X-ray fluorescence microscopy (XFM) was used to investigate the penetration of organosilicons into the wood structure. Synchrotron-based XFM with a sub-micrometer spatial resolution (μXFM) and the nanoindentation technique were also applied to examine the infiltration of cell walls by organosilicon compounds and assess their effect on the mechanical properties of the cell wall.

Due to high spatial resolution and sensitivity, multiscale synchrotron-based XFM enables mapping and quantifying trace amounts of medium- to high-Z elements in the studied object (Paunesku et al. 2006), such as Si atoms from organosilicon compounds, at different length scales across the treated wood structure. Large-field XFM has proven useful for investigating spatial localization of elements in wood at the millimeter length scale across wood block faces (Kirker et al. 2017; Zelinka et al. 2019), while an X-ray beam focused to a sub-micrometer spot size (μXFM) enables mapping of elements in the individual cell wall layers and inside wood lumina

(Jakes et al. 2015, 2020; Kirker et al. 2017). Multiscale XFM can therefore help assess if the applied organosilicons penetrated a whole wood sample evenly, as well as map and quantify organosilicon compounds that infiltrated the wood cell wall and filled cell lumina and thus, help recognize different Norimoto cell wall modification models that can aid in understanding how organosilicons stabilize waterlogged wood (Norimoto 2001).

Nanoindentation is a technique for measuring the mechanical properties of materials at a micrometer length scale; therefore, it is a suitable tool to evaluate the mechanical properties of individual wood cell walls (Wimmer et al. 1997). It has proven useful in assessing the effect of chemical infiltration on the cell wall mechanical properties in chemically modified wood (Jakes et al. 2015; Jakes and Stone 2021); it can then help to determine if the dimensional wood stabilization by organosilicons is related to reinforcement of the cell walls. Cell wall mechanical property measurements can also be useful to help identify which Norimoto molecular modifications are occurring in chemically modified cell walls (Jakes et al. 2010).

This study will provide multiscale XFM and nanoindentation characterization of organosilicon treatments applied to undegraded, chemically degraded, and biologically degraded Scots pine wood. The effects of the treatments on bulk dimensional stability will also be measured. These results will be combined with previously reported chemical and structural characteristics of the model degraded wood types used in the study (Broda et al. 2022a, b) to improve the understanding of the mechanisms by which organosilicons impart dimensional stabilization to waterlogged degraded wood. This detailed knowledge about the mechanism of wood dimensional stabilization by organosilicon compounds will help develop effective conservation treatments suited to the needs of individual waterlogged wooden artifacts of cultural heritage.

Materials and methods

Materials

This study used contemporary Scots pine (*Pinus sylvestris* L.) wood purchased from commercial timber merchants in the Wielkopolska Region, Poland. Small rectangular samples with dimensions 20 × 20 × 10 mm (radial × tangential × longitudinal direction) were cut from pine sapwood free from visible defects and subjected to chemical degradation with 50% NaOH for 3 weeks and biological decomposition using the brown rot fungus *Coniophora puteana* (Shum.: Fr.) P. Karst for 8 weeks, as previously described (Broda et al. 2022a). The choice of degradation methods was dictated by the easiness of the process under laboratory conditions and the possibility to obtain high amounts of wooden material with relatively similar degree of degradation. After degradation, the samples were immersed in distilled water to keep them filled with water, so they mimicked waterlogged wood. As a control, undegraded wood in an air-dry state was used.

Wood chemical degradation with NaOH reduced the content of lignin, hemicelluloses, and also affected crystalline cellulose, while the fungus selectively decomposed

Table 1 Selected properties of undegraded (CP), biologically degraded (BP), and chemically degraded (ChP) Scots pine wood; EMC –equilibrium moisture content at 93% RH (Broda et al. 2022a, b); ± standard deviation

Wood property	CP	BP	ChP
Mass loss (%)	–	38.5 ± 4.7	16.8 ± 1.4
Bulk density (g cm^{-3})	0.44 ± 0.02	0.44 ± 0.03	0.65 ± 0.02
Total pore volume (cm^3 g^{-1})	0.0007	0.0015	0.0012
Surface area (m^2 g^{-1})	0.36 ± 0.02	0.70 ± 0.06	0.79 ± 0.03
Cell wall density (g cm^{-3})	1.51 ± 0.002	1.54 ± 0.002	1.57 ± 0.002
Cellulose crystallinity index (%)	55.9	50.1	52.7
EMC (%)	20.3	17.7	24.6
Free hydroxyls (mmol g^{-1})	7.9 ± 0.1	8.0 ± 1	11.3 ± 0.3

Fig. 1 Air-dried pine wood samples: sound undegraded (CP), biologically degraded (BP), and chemically degraded (ChP)

cellulose and hemicelluloses (Broda et al. 2022a). More information about the structural, mechanical, and moisture parameters of undegraded and degraded model wood is presented in Table 1, and the pictures of undegraded and degraded wood can be seen in Fig. 1.

Three organosilicon compounds that have already proved effective in stabilizing wood dimensions were selected for pine treatment, including Methyltrimethoxysilane (MTMS), (3-Mercaptopropyl)trimethoxysilane (MPTMS), and 1,3-Bis-[(diethylamino)-3-(propoxy)propan-2-ol]-1,1,3,3-tetramethyldisiloxane (DEAPTMS) (Broda and Yelle 2022). Organosilicon compounds were bought from the Adam Mickiewicz University Foundation, Poznań Science and Technology Park, Poznań, Poland (Broda et al. 2020) and obtained by hydrosilylation of relevant olefins with Si–H-containing compounds in the presence of platinum catalysts (Marciniec 2009).

Methods

Wood treatment with organosilicon compounds

Wet degraded wood samples were dehydrated in 96% ethanol, during which the solution was changed 4 times. This time, based on the preliminary results, was sufficient to get good penetration of organosilicons throughout such small wooden blocks, which was confirmed by SEM + EDS analyses (Broda et al. 2020). Dehydration before the treatment helps prevent preterm polymerization of organosilicon monomers in the subsurface wood layers and facilitates more even penetration of organosilicons inside the whole specimen. Undegraded samples were used in an air-dry state. Then, wood samples were treated with 50% selected organosilicon solutions in 96% ethanol using the oscillating vacuum-pressure method and slowly air-dried after treatment, following previously described protocols (Broda et al. 2020). The bulk wood weight percent gain (WPG_{BW}) based on oven-dry masses before and after treatment, volumetric wood shrinkage (*S*v), and the volumetric anti-shrink efficiency coefficient (ASEv) were calculated according to standard equations as presented before (Broda et al. 2020) to assess the effectiveness of the impregnation and the dimensional stabilization effect of the silanes. Five specimens of each type per treatment were used, and five untreated samples of each type were used as control.

Synchrotron-based X-ray fluorescence microscopy (XFM)

Large-field view XFM Large-field view XFM was used to investigate the distribution of the organosilicon treatment throughout the wood block sample. It was performed at the 8-BM beamline at the Advanced Photon Source synchrotron at Argonne National Laboratory in Argonne, IL, USA. Experiments were performed under ambient pressure and temperature.

About 2-mm-thick radial wood sections were cut from the middle part of wood samples using a razor blade guillotine, placed between layers of 4-µm-thick 3525 Ultralene film (SPEX SamplePrep, Metuchen, NJ, USA), and mounted on a plastic holder (Fig. 2). One replicate of each variant was prepared. The X-ray beam had incident energy of 10.1 keV and was focused to a spot size of approximately 25 µm wide and high. During scanning, sections were held at a 45° offset to mitigate the self-absorption effect on the fluorescent photons. The elemental maps were built by raster scanning the focused beam across the wood section using 25 µm steps with 30 ms dwell times at each step. Quantified elemental maps were created using the XRF-Maps software (Glowacki 2020) by fitting full spectra to modified Gaussian peaks, iteratively calculating and subtracting the background, and comparing the results to standard reference materials (RF4-100-S1749, AXO DRESDEN GmbH, Heidenau, Germany). For visualization, 32-bit tiff images were exported using MAPS software (Vogt 2003).

Sub-micrometer spatial resolution XFM (µXFM) The organosilicon infiltration in the cell walls of treated pine was studied using sub-micrometer spatial resolution XFM (µXFM) at the 2-ID-E beamline at the Advanced Photon Source synchrotron

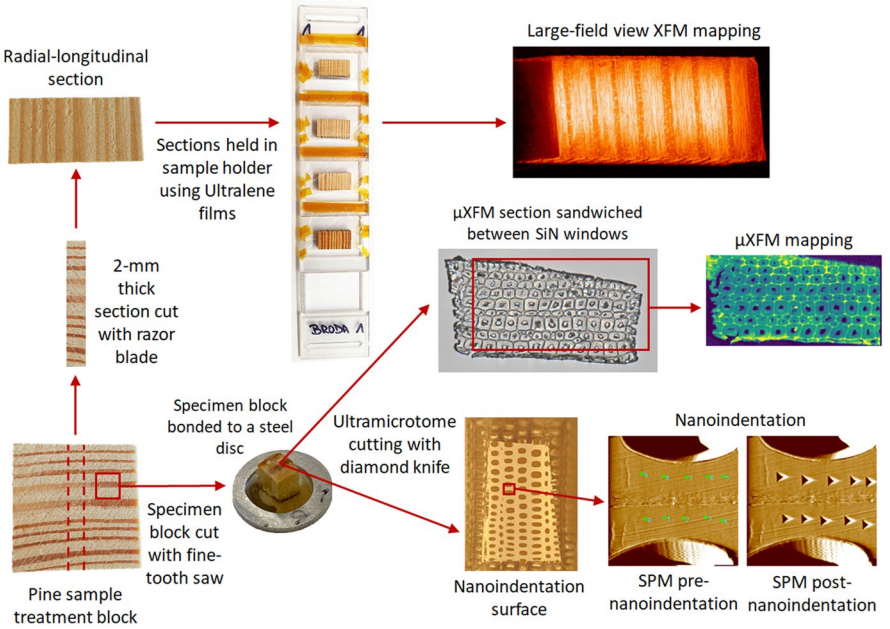

Fig. 2 Experiments scheme for large-field view X-ray fluorescence microscopy (XFM), sub-micrometer spatial resolution XFM (µXFM), and nanoindentation; XFM holder for large-field view XFM mapping contains sections from four different wood samples

at Argonne National Laboratory (Argonne, IL, USA) according to the previously described protocols (Jakes et al. 2015, 2019; Kirker et al. 2017; Broda et al. 2023). Two-µm-thick transverse wood sections were cut from latewood in small wooden blocks bonded to steel disks (Fig. 2) with a diamond knife using a Leica EM UC7 ultramicrotome (Wetzlar, Germany). For each treatment, three replicate blocks were prepared. One section from each block was carefully placed between two Norcada 200-nm-thick silicon nitride windows (Edmonton, AB, Canada) using eyelash tools and mounted on the dedicated APS 2-ID-E beamline aluminum stick sample holders. An X-ray beam with an incident energy of 10.2 keV was focused using a zone plate to a spot size of approximately 0.5 µm full width at half maximum (FWHM) in the vertical and 0.6 µm FWHM in the horizontal. Elemental maps were created by raster scanning the sample section with the focused X-ray beam using 0.5 µm step sizes and a 50 ms dwell time. The wood sections were held at a 15° angle from perpendicular to the beam to reduce the self-absorption effect of fluoresced photons. Experiments were performed under ambient pressure and temperature.

Quantified elemental maps were created using the XRF-Maps software (Glowacki 2020) by fitting full spectra to modified Gaussian peaks, iteratively calculating and subtracting the background, and comparing the results to standard reference materials (RF4-100-S1749, AXO DRESDEN GmbH, Heidenau, Germany) (Vogt 2003). Fiji image processing package (Schindelin et al. 2012) was used for data analysis and Si quantification using 32-bit tiff XFM images exported from MAPS (Vogt 2003).

Quasistatic nanoindentation

Nanoindentation was conducted using a Bruker–Hysitron (Minneapolis, Minnesota, USA) TriboIndenter® equipped with a Berkovich probe. The measurements were performed on an ultrasmooth surface in the transverse plane of each of the three replicate wood blocks from which the XFM sections were removed, as shown in Fig. 2. These nanoindentation experiments were performed during the same experimental run described in full detail before (Broda et al. 2023). In brief, quasistatic multiload nanoindentations with a maximum load of 0.30–0.45 mN were placed in the S2 cell wall layer of chosen cells. The maximum load was chosen for a given treatment to maintain similarly sized nanoindentations with maximum displacements between approximately 175 and 225 nm. The Meyer hardness (H) and nanoindentation elastic modulus (E_S^{NI}) were calculated following the protocols and analysis algorithm described in Jakes and Stone (2021). During the experiments, the specimens were conditioned under ambient pressure inside the nanoindenter enclosure at $50 \pm 1\%$ relative humidity (RH), and the temperature varied between 25 and 34 °C. The RH control is important because mechanical properties of wood cell walls are known to be sensitive to their moisture content (MC) (Yu et al. 2011). The large temperature variation was caused by issues controlling the temperature in the laboratory housing the nanoindenter. However, the temperature variation was not expected to substantially affect the results because the RH was maintained over the different temperatures, which means that the wood cell wall MC was not expected to vary by more than 0.3% over the temperature variations (Glass and Zelinka 2021). After following established analysis protocols (Jakes and Stone 2021), no H nor E_s^{NI} data exhibited an indentation size effect and for each treatment results from each unloading slope were grouped together to calculate averages, standard deviations, and standard errors. The standard errors were used to represent the measurement precisions and to aid in determining differences between treatments (Jakes and Stone 2021; Broda et al. 2023).

Results

Effect of organosilicon treatment on dimensional stability

The effectiveness of pine wood impregnation by selected organosilicon compounds expressed as bulk wood weight percent gain (WPG_{BW}) is presented in Table 2. A clear correlation between the degree of wood degradation and the level of impregnation can be seen – the higher the mass loss in Table 1, the higher the WPG_{BW} values. Biologically degraded wood (BP), which had a mass loss of about 38.5%, had the highest WPG_{BW} values between 54 and 64%. With a mass loss of about 17%, chemically degraded wood (ChP) had WPG_{BW} values between 42 and 53%. The lowest WPG_{BW} values were recorded for contemporary undegraded wood (CP), ranging from 26 to 33%. This agrees with previous work showing that an increase in the degree of wood degradation facilitates the penetration of higher amounts of applied chemicals (Broda et al. 2019b, 2021).

Table 2 Bulk wood weight percent gain (WPG_{BW}), volumetric shrinkage (S_v), and volumetric anti-shrink efficiency (ASE_v) for pine wood – sound undegraded (CP), biologically degraded (BP), and chemically degraded (ChP), untreated (*c*), and treated with Methyltrimethoxysilane (MTMS) (1), treated with (3-Mercaptopropyl) trimethoxysilane (MPTMS) (2), and treated with 1,3-Bis-[(diethylamino)-3-(propoxy)propan-2-ol]-1,1,3,3-tetramethyldisiloxane (DEAPTMDS) (3); ± standard deviation

Sample	WPG_{BW} (%)	S_v (%)	ASE_v (%)
CPc	–	–	–
CP1	26 ± 5	− 0.2 ± 0.2	–
CP2	33 ± 6	− 2.1 ± 0.7	–
CP3	31 ± 6	− 0.7 ± 0.3	–
BPc	–	22.3 ± 0.9	–
BP1	54 ± 8	4.6 ± 0.2	79
BP2	63 ± 4	4.0 ± 1.3	82
BP3	64 ± 3	5.5 ± 0.3	75
ChPc	–	25.5 ± 3.8	–
ChP1	41 ± 6	12.3 ± 1.7	52
ChP2	53 ± 5	6.5 ± 1.6	75
ChP3	51 ± 5	6.6 ± 2.4	74

Regardless of the wood degradation type and degree, treatment with MTMS resulted in the lowest WPG_{BW} values, while treatments with MPTMS and DEAPTMDS were more effective, reaching WPG_{BW} values about 6–12 percentage points higher than the MTMS treatment. The observed trend in the retention level of applied organosilicons in wood is consistent with our previous research on chemically degraded pine wood and archeological oak wood (Broda and Plaza 2023; Broda et al. 2023). However, it differs from the results obtained for highly degraded elm wood with a mass loss of about 70–80%. In the highly degraded elm wood, the highest WPG_{BW} was obtained for treatment with MTMS, then for DEAPTMDS, and the lowest for MPTMS treatment (Broda et al. 2019a, 2020; Broda and Yelle 2022). This suggests that the impregnation effectiveness depends not only on the type of organosilicon but also on other factors, including wood species and the degree and type of wood degradation.

Compared to the sound undegraded pine control CPc, BPc and ChPc had volumetric shrinkages of 22.3 and 25.5%, respectively. Treatments of CPc caused slight swelling of about 0.2–2.1%, while in degraded wood, the impregnation with organosilicons resulted in increased dimensional stability during drying (Table 2). The treatments were generally more effective in stabilizing the dimensions of the more degraded BP samples than the ChP ones, which likely follows from the higher WPG_{BW} in BP than ChP. Volumetric wood shrinkage decreased from about 22% for BPc wood to 4.0%, 4.6%, and 5.5% for MPTMS-, MTMS-, and DEAPTMDS-treated wood, respectively, while for ChP wood, it decreased from 25.5% for ChPc to about 6.5% for MPTMS- and DEAPTMDS-treated samples, and only 12.3% for MTMS-treated sample. Based on the volumetric wood shrinkage values, the highest anti-shrink efficiency was calculated for MPTMS and MTMS treatment of BP (82 and 79%, respectively), and slightly lower values were obtained for DEAPTMDS treatment of BP and ChP wood (75 and 74%, respectively), as well as MPTMS treatment of ChP samples (75%). The lowest anti-shrink efficiency of 52% was observed for MTMS-treated ChP.

The trend in the stabilizing effect expressed as ASE_V values for organosilicon treatments observed for ChP wood (MPTMS 75%, then DEAPTMDS 74%, and MTMS 52%) is in line with our data reported for highly degraded waterlogged elm wood treated with the same chemicals (MPTMS 98–99%, then DEAPTMDS 89.5–92%, and MTMS 80.5–82%) (Broda et al. 2019a, 2020; Broda and Yelle 2022). For biologically degraded pine wood (BP), the stabilizing effectiveness of MPTMS treatment was the highest, while that of MTMS was higher than that of DEAPTMDS (ASE of 82%, 79%, and 75%, respectively). Interestingly, for less degraded archeological oak excavated from the ground, the trend was different, with ASE_V for MPTMS almost two times lower than for MTMS and DEAPTMDS (ASE of 61%, 55%, and 36% for treatment with MTMS, DEAPTMS, MPTMS, respectively) (Broda et al. 2023). These results show that the stabilizing effect of organosilicons is not universal and presumably depends on the wood species and the related anatomical features, wood structure, degree of degradation, and chemical composition, which will be important from the conservation perspective when choosing preservation treatments.

Multiscale XFM mapping of Si in wood

Large-field view XFM Si maps enabled observations of the distribution of organosilicons in the treated undegraded and degraded pine wood blocks. Compared to the untreated blocks (Fig. 3a–c), blocks treated with organosilicons (Fig. 3d–l) had much higher Si intensities, which indicated that organosilicons penetrated the wood blocks from which these 2-mm-thick sections were cut (Fig. 2). A more detailed interpretation of the Si maps in Fig. 3 is aided by further explanation of the XFM experiments. The Si maps were created by raster scanning an approximately 25 µm diameter X-ray beam across the surface of a 2-mm-thick wood section. At each position, the incident 10.1 keV X-ray beam is expected to penetrate most of the way through the 2-mm-thick specimen, creating an interaction volume that includes both the cell wall and lumina. However, fluoresced photons created in this interaction volume will only be measured if they escape the wood and reach the detector. Si Kα fluoresced photons, which have a relatively low 1.84 keV energy, will be more readily absorbed by the wood cell wall material than the higher energy incident 10.1 keV X-ray beam. Assuming a cell wall density of 1.5 g cm^{-3} and an average $C_4H_{10}O_3$ molecular formula, it can be calculated that about 60% of Si Kα fluoresced photons will be absorbed after passing through only 10 µm of cell wall material (Henke et al. 1993). This absorption by the wood cell walls means that only Si within the first 5–10 cells from the surface can be effectively detected. Furthermore, the observed Si map will be affected by the geometry of the experimental set-up. As shown schematically in Fig. 4, the sample was held at a 45° offset to the beam to mitigate the self-absorption effect on the fluorescent photons. At X-ray beam position #1 on the front end of the block, the path to the detector is blocked by the corner of the sample, and very few Si Kα fluoresced photons were expected to be detected because the Si Kα photons fluoresced toward the detector were absorbed by the wood. This effect can be observed on the left-hand sides of the Si maps in Fig. 3. While some fluoresced

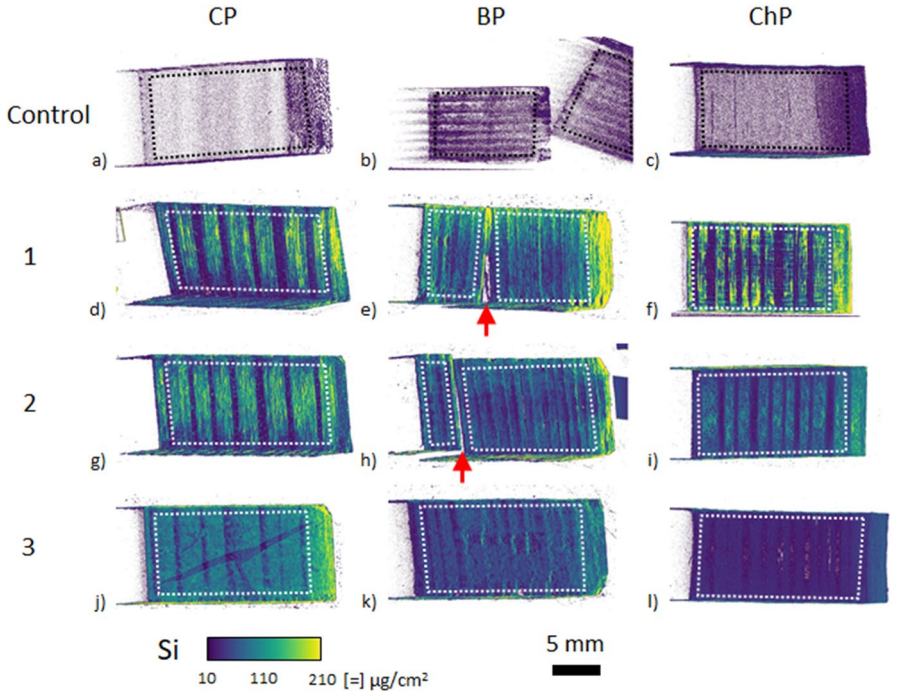

Fig. 3 Large-field view XFM maps showing localization of Si ions in 2-mm-thick pine wood sections – sound undegraded (CP), biologically degraded (BP), and chemically degraded (ChP), untreated (Control), and treated with Methyltrimethoxysilane (MTMS) (1), treated with (3-Mercaptopropyl)trimethoxysilane (MPTMS) (2), and treated with 1,3-Bis-[(diethylamino)-3-(propoxy)propan-2-ol]-1,1,3,3-tetramethyldisiloxane (DEAPTDMS) (3). The areas enclosed by dashed lines indicate areas least affected by the sample and experimental geometries and should be used for comparisons. The BP blocks were weak and fractured. The **b** control BP block fell apart during scanning, and the left-hand side rotated 90°. Arrows indicate cracks in the **e** and **h**

photons reach the detector at the top and bottom edges, most are absorbed, and there is very little Si detected when the beam is located on the front end of the specimen in position #1. When the beam is at the opposite end, position #3 in Fig. 4, there were more fluoresced photons because fluoresced photons from the back end also have a free path to the detector and can add to the measured signal. Some blocks were also inadvertently tilted up or down slightly, such as Fig. 3d, in which the block was tilted up. Therefore, interpretation should be confined to the areas on the front block face away from the edges, as indicated by position #2 in Fig. 4 and the area enclosed by the dashed lines in Fig. 3. Areas near edges and cracks in specimens need to be excluded. Over the regions enclosed by dashed lines, the Si maps are 2D area projections of a 3D volume measurement that should be consistent, and comparisons between these areas should be minimally affected by the sample edges and experimental set-up.

The earlywood and latewood bands are evident in Fig. 3 Si intensity maps. Except for the BP control block (Fig. 3b), the wood blocks were oriented with their

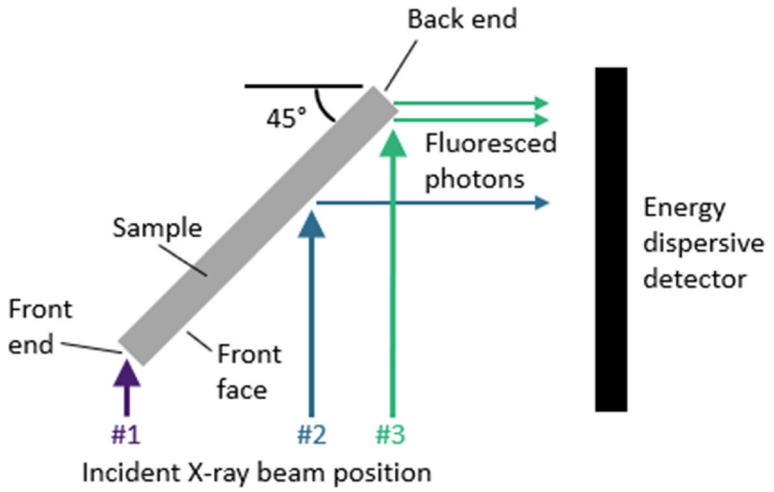

Fig. 4 Top-down schematic view of a 2-mm-thick wood section in the large-field view XFM beamline

longitudinal directions vertical, and the bands are evident as vertical stripes. The BP control block (Fig. 3b) fell apart and shifted in the Ultralene envelope before scanning. The longitudinal direction was horizontal in the left-hand piece and was approximately 30° in the right-hand piece. For all these wood blocks, the latewood bands can be identified as the thinner stripes in the Si maps because the latewood bands were much thinner than the earlywood bands. For treated samples, a higher Si intensity was observed in earlywood than in latewood. Within earlywood or latewood for a given treated block, no obvious effect of proximity to edges is observed within the dashed lines, which indicates the organosilicon treatments distributed throughout the block during treatment. However, some inhomogeneity in Si intensity can be observed, especially in the earlywood for the MTMS- and MPTMS-treated blocks. Because MTMS and MPTMS can self-polymerize, these higher-intensity regions in the earlywood may indicate areas of polymerized organosilicon in the earlywood tracheid lumina. The DEAPTDMS-treated samples were found to have some residual liquid on their surface, which caused the Ultralene film to adhere in some places to the sticky surface. This accumulated liquid and film sticking to the surface likely caused the inhomogeneous features in the DEAPTDMS-treated samples (Fig. 3j–l).

The higher Si intensity in the earlywood signifies that more fluoresced photons from Si reached the detector when the X-ray beam probed the earlywood. However, it is not straightforward to interpret the higher intensity with regard to organosilicon treatment. Compared to latewood, earlywood is less dense because it has thinner cell walls and larger lumina. Again, assuming a cell wall density of 1.5 g cm^{-3} and average $C_4H_{10}O_3$ molecular formula, about 35 or 60% of Si Kα fluoresced photons would be absorbed going through 5 or 10 µm of cell wall material, respectively (Henke et al. 1993). Given that double cell walls are about 5 µm thick in earlywood and 10 µm thick in latewood, fluoresced photons from Si in lumina deeper into the

scanned front face have a much higher probability of reaching the detector in earlywood than latewood. If the organosilicon only infiltrated in the cell wall material and did not deposit in the lumina, then, a minimal difference in Si intensity between earlywood and latewood bands would have been expected, assuming that the amount of infiltration was consistent between the cell walls in earlywood and latewood. However, the higher Si intensity suggests either that the organosilicon is in the lumina or that the earlywood cell walls have more organosilicon. The higher spatial resolution experiments of 2-µm-thick sections will provide more insights.

Analysis of µXFM Si maps (Figs. 5, 6 and 7) of 2-µm-thick sections enabled studying the organosilicon infiltration in the microstructure of treated pine latewood. In these thin sections, the incident X-ray beam completely penetrated the wood section, and there was much less cell wall to absorb the fluoresced photons. The total fluorescence yield (TFY) images of the controls (Figs. 5a, 6a, and 7a) revealed the cellular microstructure and a few effects of the biological and chemical degradations on the microstructure. The BPc secondary cell walls were damaged during sectioning with the secondary cell walls and sometimes appeared to peel away from the compound middle lamella, which indicated a substantial level of degradation caused by the decay fungus at the interface between the secondary cell walls and compound middle lamella. There are no maps of DEAPTDMS-treated samples for BP wood because the specimens were too degraded, and the treatment caused the specimen to be wet and sticky, which prevented cutting the intact 2-µm-thick transverse wood sections necessary for µXFM measurements. The chemical degradation also seemed to modify the shapes of the cells, with lumina sizes decreasing and changing shape. The smaller lumina was consistent with the increase in bulk wood density measured for ChP (Table 1).

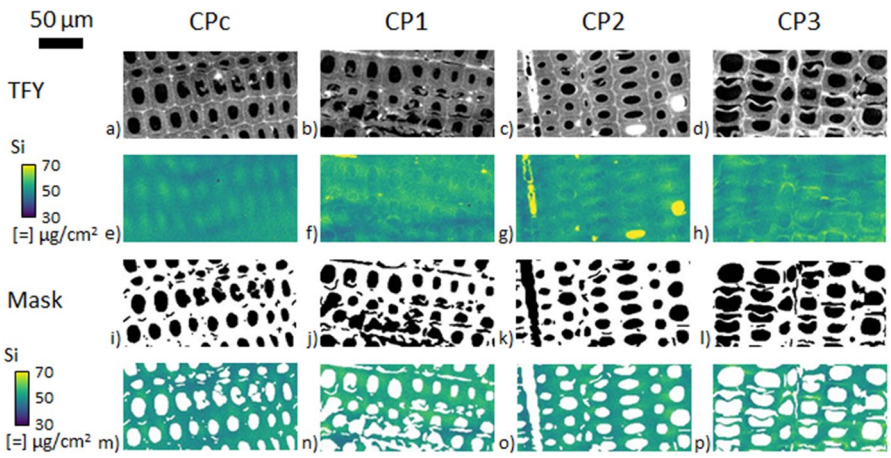

Fig. 5 Micro XFM maps showing localization of Si ions in sound undegraded pine wood (CP), untreated (*c*), and treated with Methyltrimethoxysilane (MTMS) (1), treated with (3-Mercaptopropyl)trimethoxysilane (MPTMS) (2), treated with 1,3-Bis-[(diethylamino)-3-(propoxy)propan-2-ol]-1,1,3,3-tetramethyldisiloxane (DEAPTMDS) (3). Total fluorescence yield (TFY) maps were included to visualize the wood cell structure

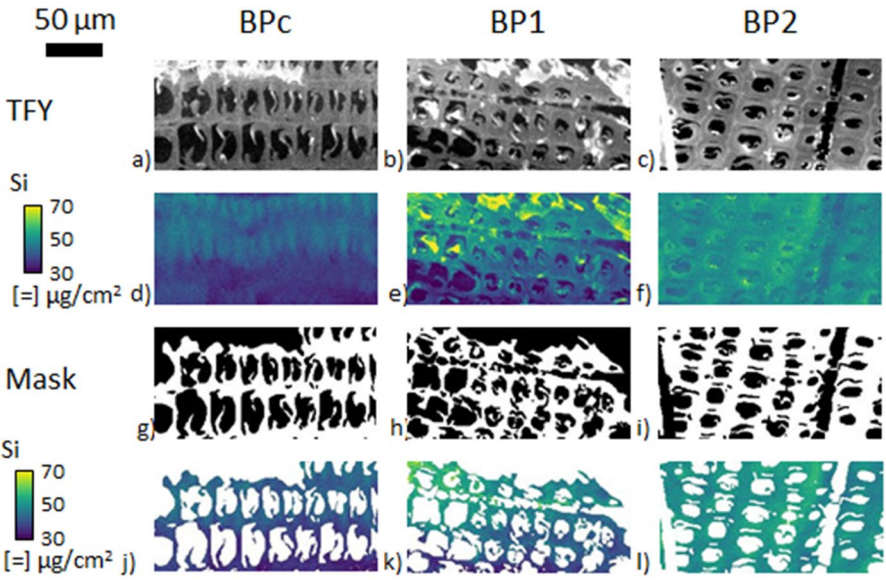

Fig. 6 XFM maps showing localization of Si ions in biologically degraded pine wood (BP), untreated (*c*), and treated with Methyltrimethoxysilane (MTMS) (1), treated with (3-Mercaptopropyl)trimethoxysilane (MPTMS) (2). Total fluorescence yield (TFY) maps were included to visualize the wood cell structure

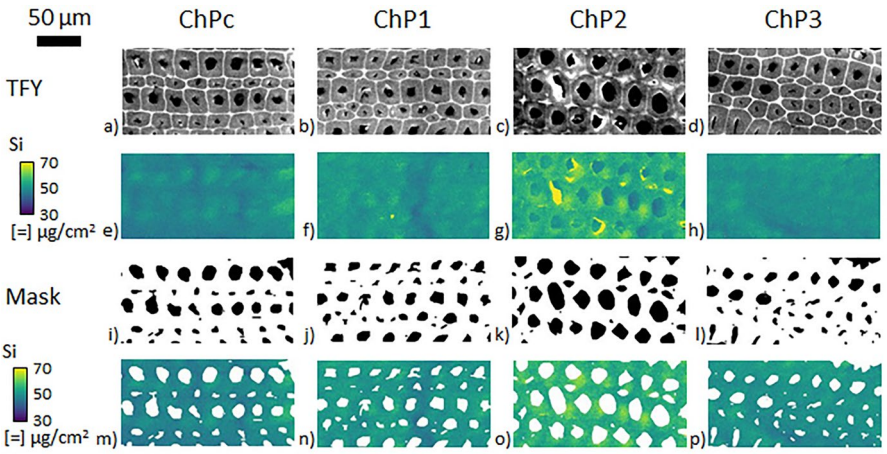

Fig. 7 XFM maps showing localization of Si ions in chemically degraded pine wood (ChP), untreated (*c*), and treated with Methyltrimethoxysilane (MTMS) (1), treated with (3-Mercaptopropyl)trimethoxysilane (MPTMS) (2), treated with 1,3-Bis-[(diethylamino)-3-(propoxy)propan-2-ol]-1,1,3,3-tetramethyldisiloxane (DEAPTMDS) (3). Total fluorescence yield (TFY) maps were included to visualize the wood cell structure

In the Si maps of control specimens (Figs. 5e, 6d, 7e), the Si intensity of the cell walls was lower than the lumina. This is due to the large Si signal coming from the SiN windows and the low amount of Si in untreated wood. Because the wood cell wall absorbs about 15% of the Si Kα photons fluoresced from the SiN window behind the wood sections, the measured Si intensity will be lower in regions with cell walls when the cell wall does not have a large amount of Si (Broda et al. 2023). In treated wood, specimens that had obviously higher Si intensity in the cell walls, as indicated by cell walls with higher Si intensities than in the lumina, included CP1 (Fig. 5f), BP1 (Fig. 6e), BP2 (Fig. 7f), and ChP2 (Fig. 7g). Some Si hot spots are visible in samples treated with MTMS and MPTMS (yellow spots with Si intensities greater than 60 µg cm^{-2} in Figs. 5f and g, 6e and f, 7f and g, respectively). They can be seen mainly in the cell lumina and other micrometer-scale cavities in the wood structure and on the cell wall surface in the lumina, which indicates that organosilicons penetrated the open areas and polymerized there.

In all treated samples, there was visual evidence that the Si intensity was higher than in untreated ones (Figs. 5, 6, and 7). However, visual observation of Si XFM maps did not allow for accurate quantification of differences in Si content in the cell walls of different samples. Therefore, to enable quantification, which is necessary to understand better the stabilizing mechanism of organosilicon compounds in wood, masks that only included well-defined cell wall material were manually created using the Fiji image software (Figs. 5i–l, 6g–i, and 7i–l). Exemplary masked Si maps that served for quantification of Si content in cell walls are presented in Figs. 5m–p, 6j–l, and 7m–p, and the resulting averages of values obtained from three sections per wood type and treatment are presented in Table 3. The Si intensity arising from the organosilicon treatment was estimated for each wood type by subtracting the Si intensity from the cell wall mask in the corresponding control cell wall from the Si intensity in the treated cell wall. This assumed that the increased Si intensity in the treated cell walls could be entirely attributed to infiltrated organosilicons (Broda et al. 2023). The values of Si intensity due to the treatment in Table 3 show that all organosilicons applied infiltrated cell walls of all wood types used in the study. However, the average infiltration varied between the types of wood degradation and organosilicon treatment.

To get a better understanding of the organosilicon penetration into the wood, Table 3 also includes their cell wall weight percent gain (WPG_{CW}), weight gain per cell wall volume (OG_{cw}), and the number of organosilicon molecules per cell wall volume (Nm), which were calculated as described in Broda et al. (2023). Briefly, the calculations were made using the Si intensity value due to the treatment (Table 3), the molecular formulae of the organosilicons (MTMS – $CH_3Si(OCH_3)_3$, MPTMS – $HS(CH_2)_3Si(OCH_3)_3$, and DEAPTMDS – $[(C_2H_5)_2NCH_2CH(OH)CH_2O(CH_2)_3Si(CH_3)_2]_2O$), the molecular masses of the organosilicons (MTMS – 136.22 g mol^{-1}, MPTMS – 196.34 g mol^{-1}, and DEAPTMDS – 508.88 g mol^{-1}), known µXFM section thickness, and an assumed cell wall density of 1.45 g cm^{-3}. The calculations also assume that organosilicon molecules are in their monomer form, and we are ignoring the potential changes in their masses due to reactivity with wood polymers or other monomers. Because the different organosilicons have different numbers of Si atoms and different molecular weights, comparing WPG_{CW},

Table 3 Bulk wood weight percent gain (WPG_{BW}), the Si intensity from the cell wall mask, the Si intensity due to the treatment, calculated cell wall weight percent gain (WPG_{CW}), organosilicon weight gain per cell wall volume (OG_{cw}), and the number of organosilicon molecules that infiltrated the cell wall (Nm) of pine wood – sound undegraded (CP), biologically degraded (BP), and chemically degraded (ChP), untreated (c), and treated with Methyltrimethoxysilane (MTMS) (1), treated with (3-Mercaptopropyl)trimethoxysilane (MPTMS) (2), and treated with 1,3-Bis-[(diethylamino)-3-(propoxy)propan-2-ol]-1,1,3,3-tetramethyldisiloxane (DEAPTMDS) (3); ± standard deviation; Si intensities were the averages of the masked map regions from the three sections for each sample

Sample	WPG_{BW} (%)	Si intensity from the cell wall mask (μg cm^{-2})	Si intensity due to the treatment (μg cm^{-2})	WPG_{CW} (%)	OG_{cw} (g cm^{-3})	Nm (mmol cm^{-3})
CPc	–	51.6	0	–	–	–
CP1	26.2 ± 5.1	53.8	2.2	3.54	0.0513	0.4
CP2	32.7 ± 5.6	53.4	1.9	4.32	0.0627	0.3
CP3	31.2 ± 5.7	54.5	2.9	8.76	0.1271	0.2
BPc	–	44.6	0	–	–	–
BP1	53.6 ± 7.6	49.8	5.2	8.36	0.1212	0.9
BP2	63.3. ± 4.2	52.1	7.4	17.35	0.2515	1.3
BP3	64.0. ± 3.2	–	–	–	–	–
ChPc	–	48.5	0	–	–	–
ChP1	41.5 ± 5.6	49.1	0.7	1.08	0.0156	0.1
ChP2	53.2 ± 4.8	54.6	6.1	14.29	0.2072	1.1
ChP3	51.5 ± 4.7	50.8	2.4	7.14	0.1036	0.2

Example masks are shown in Figs. 4m–p, 5j–l, and 6m–p

OG_{CW}, and Nm is more physically meaningful than the Si intensities from the XFM maps.

The results presented in Table 3 show that the values of WPG_{CW} are significantly lower than WPG_{BW} in Table 2. For all wood types, WPG_{CW} values were about 3.5–7.5 times lower than WPG_{BW} except for the outlier of MTMS-treated ChP, which was about 40 times lower. The lower WPG_{CW} is consistent with our recent archaeological oak results (Broda et al. 2023), which revealed about 5–9 times lower values for WPG_{CW} than WPG_{BW}. The consistently higher WPG_{BW} values indicated that substantial amounts of organosilicon did not infiltrate the cell walls and likely polymerized in the open spaces of the cellular structure, such as the partially or fully organosilicon-filled lumina observed in Figs. 5g and 7g. The inhomogeneous distribution of the Si intensity in the earlywood of the large-field view XFM maps (Fig. 3) also supports that the organosilicons polymerize in the open spaces of the cellular structure. For MTMS-treated ChP (Fig. 3f), there are some particularly high Si intensities in the earlywood, and the latewood Si intensity is relatively low, which indicates that for ChP, the MTMS impregnated the earlywood better than the latewood. Because the WPG_{CW} measurements were made on latewood, this may explain why the ratio of WPG_{BW} to WPG_{CW} had the outlier value of 40.

For a given treatment between wood types, WPG_{CW} was higher in BP than CP or ChP. This trend was similar to the observation that BP had the highest WPG_{BW}

values. Physical properties in Table 1 that may explain this trend include the total pore volume, surface area, and cell wall density. BPc had the highest reported total pore volume and surface area, but a cell wall density that was higher than CPc and lower than ChPc (Table 1). The total pore volume was calculated from nitrogen absorption experiments and represents the total measure volume of pores measured with diameters between 4 nm and approximately 73 nm (Broda et al. 2022a). The observation that the total pore volume and cell wall density do not directly correlate with higher pore volumes causing lower densities indicates the likely presence of pores not being measured by nitrogen absorption that were influencing cell wall density measurements. Based on these results, the total pore volume and surface area correlated better than cell wall density to indicate cell walls with higher accessibility for the organosilicons to infiltrate them.

For all wood types, higher WPG_{cw} values were calculated for MPTMS and DEAPTDMS treatments than for MTMS. In our previous research on archeological oak treated with the same three organosilicons, however, the WPG_{cw} results were different. The highest WPG_{cw} value was observed for DEAPTDMS-treated samples, while for wood treated with MTMS and MPTMS, WPG_{cw} was about 50% lower (Broda et al. 2023). It remains unclear why MTMS and MPTMS did not infiltrate the ChP cell walls as much as in the BP. Since it is known that due to NaOH treatment Na ions infiltrate cell walls and interact with cellulose microfibrils (Nishiyama et al. 2000; Cai et al. 2015), it may be that the ions presence in the ChP cell walls somehow limited the cell wall infiltration by organosilicons. Future cell wall chemical analyses should provide additional insights.

The number of organosilicon molecules per cell wall volume (Nm) is reported because it could provide additional insights into how many potential chemical reactions are forming with wood polymer and the potential formation of an organosilicon interpenetrating polymer network (IPN). Likely, an IPN will not form until some threshold numbers of monomers are able to infiltrate the cell wall. The highest Nm values were obtained for MPTMS-treated degraded wood (about 1.3 and 1.1 mmol per cm^{-3} for BP and ChP, respectively) and MTMS-treated degraded BP and undegraded CP samples (about 0.9 and 0.4 mmol per cm^{-3}, respectively). The lowest values were obtained for DEAPTMDS-treated CP samples (approximately 0.2 mmol per cm^{-3}) and MTMS-treated ChP specimens (only about 24 mmol per cm^{-3}). For CP, the results are similar to those reported for well-preserved low-permeable archeological oak wood, with the highest amount of MTMS molecules per cell wall volume, then MPTMS and DEAPTMDS (290, 260, and 180 micromoles per cm^{-3}, respectively), which reflects the differences in molecular mass and sizes of chemicals applied (Broda et al. 2023).

Cell wall mechanical property measurements

Nanoindentation measured the elastic modulus (E_s^{NI}) and Meyer's hardness (H) of the S2 secondary cell wall layer in the longitudinal direction for undegraded and degraded pine wood untreated and treated with organosilicons (Table 4). Considering wood type, the highest E_s^{NI} was recorded for undegraded CPc wood, while

Table 4 Nanoindentation elastic modulus (E_s^{NI}) and hardness (H) results for pine wood – sound undegraded (CP), biologically degraded (BP), and chemically degraded (ChP), untreated (c), and treated with Methyltrimethoxysilane (MTMS) (1), treated with (3-Mercaptopropyl)trimethoxysilane (MPTMS) (2), treated with 1,3-Bis-[(diethylamino)-3-(propoxy)propan-2-ol]-1,1,3,3-tetramethyldisiloxane (DEAPT-MDS) (3); N – number of multiload nanoindentations, n – number of unloading segments analyzed, Std. dev. – standard deviation, Std. er. – standard error

Sample	N	n	Elastic modulus, E_s^{NI}			Hardness, H		
			Average (GPa)	Std. dev. (GPa)	Std. er. (GPa)	Average (MPa)	Std. dev. (MPa)	Std. er. (MPa)
CPc	56	498	16.4	1.5	0.1	389	27	1
CP1	70	605	15.4	2.2	0.1	401	39	2
CP2	68	569	16.4	1.1	0.0	428	22	1
CP3	48	335	16.1	1.1	0.1	370	22	1
BPc	64	557	15.3	2.2	0.1	395	31	1
BP1	58	509	13.8	2.3	0.1	388	43	2
BP2	75	620	15.7	1.2	0.0	448	25	1
BP3	56	487	11.5	4.0	0.2	260	86	4
ChPc	75	668	13.8	2.8	0.1	358	44	2
ChP1	75	675	13.3	1.1	0.0	351	24	1
ChP2	71	639	11.7	0.7	0.0	327	13	1
ChP3	47	423	11.7	1.9	0.1	267	44	2

biological and chemical degradation processes decreased E_s^{NI} by about 7 and 16%, respectively. CPc and BPc had similar H values, whereas, in ChPc, the H value decreased by about 8%. Differences in moisture content (MC) likely accounted for much of the decrease in E_s^{NI} and H in ChPc secondary cell walls. Under the 50% RH conditions inside the nanoindenter enclosure, the MC of CPc and BPc is reported to be about 7.5% MC, and ChPc is 10% MC (Broda et al. 2022b). For nanoindentation experiments in the S2 secondary cell wall of Masson pine, this modest 2.5% increase in MC caused a decrease of about 6% in Es^{NI} and 10% in H (Yu et al. 2011). A similar plasticization effect would be expected in the ChPc cell walls. Taking into consideration these moisture effects, the measured mechanical properties of the S2 layer cell walls remained relatively unchanged after degradation despite the large 17 and 38% mass losses for ChPc and BPc, respectively. This small change in mechanical properties is not surprising, considering the cell wall densities and cellulose crystallinity index remained relatively unchanged after degradation (Table 1). Collectively, these results indicate that as polymers are removed from the wood cell walls during degradation, substantial pores that could affect mechanical properties are not being formed in the cell wall, but rather the remaining cell wall polymers recoalesce during drying to reform a solid material with similar properties to the CPc cell walls.

The nanoindentation results showing BPc had higher mechanical properties than ChPc contradicted viscoelastic measurements of bulk wood in which CPc and ChPc have similar storage moduli, and the storage modulus for BPc decreased by about 45% (Broda et al. 2022b). Based on the observations of the secondary cell walls often peeling away from the compound middle lamella in the 2-µm-thick cell walls

(Fig. 6a–c), it appears that the brown rot fungus weakened the interfaces between neighboring cells. This weakened interface likely caused the bulk wood properties to decrease substantially. However, the nanoindentation measurements revealed that the mechanical properties of the secondary cell walls were much less affected. Given the observations in Fig. 6b and c that the secondary cell walls continued to peel away even after MTMS and MPTMS treatments and in Fig. 3e and h showing the 2-mm-thick sections still fractured after treatment, it seems unlikely that these treatments would effectively restore the mechanical properties of BPc at the bulk wood level.

Organosilicon treatments affected the cell wall E_s^{NI} and H differently depending on the wood type and treatment. For all types of wood, DEAPTMDS plasticized the cell walls, causing decreases in both E_s^{NI} and H. It is known that organosilicons, especially when not fully polymerized, can have a plasticizing effect on various materials (Wang and Bonfield 2001; Sae-oui et al. 2006; Bengtsson and Oksman 2006; Hayeemasae et al. 2023). DEAPTMDS is a hydrophilic siloxane that cannot polymerize, and its interactions with wood polymers are limited to the formation of hydrogen bonds via amino groups (Popescu and Broda 2021), hence its observed plasticizing effect on wood. The plasticization was much stronger in the BP and ChP than in the CP. DEAPTMDS plasticization in BP and ChP cell walls were the strongest effects observed by nanoindentation, with a 15–25% decrease in E_S^{NI} and a 25–34% decrease in H. Although DEAPTMDS WPG_{CW} could not be measured for BP, the WPG_{CW} for CP and ChP was 9 and 7%, respectively. The similar values of WPG_{CW} and decrease in cell wall mechanical properties indicated that degradation at the molecular level in ChP occurred and resulted in cell walls with a molecular structure that was more easily plasticized by DEAPTMDS than the native molecular structure in CP cell walls. We know that fungal decay and alkali treatment caused degradation of hemicelluloses in BP and ChP (Broda et al. 2022a). Hemicelluloses are often viewed as a mechanical bridge between cellulose fibrils and lignin (Salmén and Burgert 2009), so breaking that bridge may have facilitated the increased cell wall plasticization by DEAPTMDS.

Effects of the MTMS and MPTMS treatments on nanoindentation properties were not as consistent across wood types nor as strong as for DEAPTMDS treatments. MTMS modestly decreased E_s^{NI} and H for all wood types except for CP H, which increased slightly. After MPTMS treatment, E_s^{NI} and H stayed constant or increased for CP and BP but decreased for ChP. These differences in behavior likely indicated that the treatments interacted with the different wood types differently. These interactions could include changing the wood cell wall hygroscopicity or molecular structure. We know that MTMS treatment decreases wood hygroscopicity (Tshabalala et al. 2003; Broda et al. 2018a, 2021; Tang et al. 2023), which should decrease the plasticizing effect of water on wood and increase mechanical properties. However, a plasticizing effect of MTMS treatment has been observed for archeological oak and elm wood (Broda et al. 2021), which probably resulted from the incomplete polymerization of MTMS monomers inside the wood structure as observed during the measurement of hygroscopic properties of MTMS-treated wood (Broda et al. 2018a). The decreases in nanoindentation properties for MTMS-treated wood suggest that the plasticization effect from MTMS monomers was stronger. As

for MPTMS, it can polymerize readily due to the presence of alkoxy groups, similar to MTMS (Donath et al. 2004; Xie et al. 2010); it also strongly reacts with wood via alkoxy and mercapto groups (Tshabalala et al. 2003; Sèbe et al. 2004; Xie et al. 2010; Popescu and Broda 2021) and decreases wood hygroscopicity (Broda et al. 2018a), which may explain the increase on the mechanical properties of CP and BP wood treated with MPTMS.

The obtained results here for model pine degraded pine are different from what we reported for archeological oak treated with the same organosilicons. For E_s^{NI}, all treatments resulted in an increase in elastic modulus by 19%, 21%, and 27% for MTMS, MPTMS, and DEAPTMDS, respectively (Broda et al. 2023). For H, MTMS and MPTMS caused 5% and 16% increases, whereas DEAPTMDS caused a 4% decrease.

In summary, the effect of organosilicon treatment on the mechanical properties of wood cell walls evidently depends on the type of wood treated and organosilicon, the amount of cell wall infiltration, and molecular scale interactions between the organosilicons and wood polymers.

Discussion

Conservation of highly degraded waterlogged archaeological wood requires consolidants that prevent catastrophic shrinkage that can lead to the complete disintegration of the wooden artifact as it dries. The consolidants must also maintain or improve the mechanical integrity of the archaeological wood to conserve it for display and study under ambient conditions outside of water. Although organosilicon consolidants have shown promise for the conservation of waterlogged archaeological wood, additional study is needed to improve them further. In this research, we utilized model degraded wood because of the limited amount of precious archaeological wood available. The model degraded wood was treated with MTMS, MTPMS, or DEAPTMDS to understand better the mechanisms by which organosilicons can act as appropriate consolidants. The cell wall and molecular wood modification models in Figs. 8a and b are useful to facilitate the discussion of these mechanisms. In waterlogged wood, water infiltrates both the cell wall and cell lumina (model A5) (Grattan 1987). Water also swells wood at the molecular level but does not react with wood polymers (model B4). For a consolidant to stabilize the dimensions of the wood as it dries, it must replace whatever water necessary to prevent excessive wood shrinkage as water evaporates (Grattan 1987), which may include filling the cell lumina (model A4) or infiltrating the cell walls (models A2, A3, or A5) and swelling it at the molecular scale (B2, B3, B4, or B5). XFM and nanoindentation experiments were performed to help identify the roles in which these cell walls and molecular modifications contributed to the dimensional stabilization of organosilicon-treated wood.

Both the μXFM results (Table 3) and nanoindentation results (Table 4) support that MTMS, MTPMS, and DEAPTMDS infiltrated and modified cell walls in all three types of wood treated in this study. The μXFM was used to measure WPG_{CW} of 1–17% after organosilicon treatment**.** The nanoindentation revealed

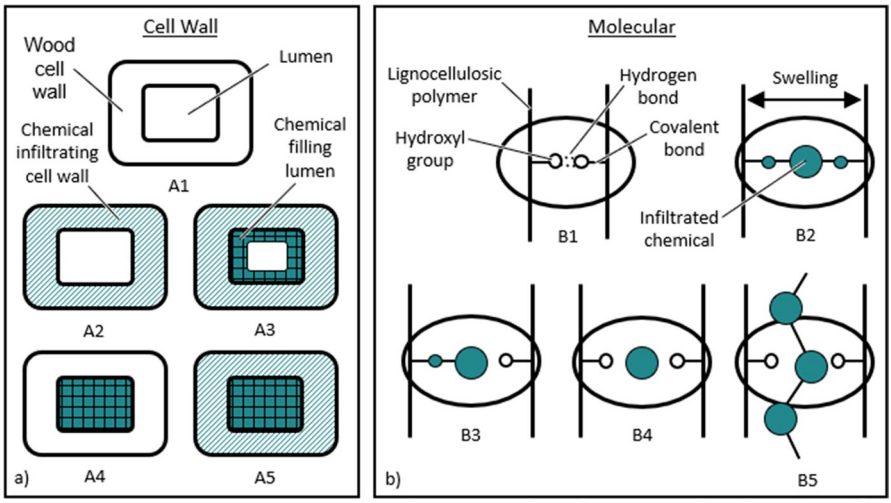

Fig. 8 Norimoto **a** cell wall and **b** molecular wood modification models (Norimoto 2001). The unmodified cell wall model (A1) includes the wood cell wall and empty lumen. Potential modifications at the cell wall level include (A2) chemicals only infiltrating the cell wall, (A3) chemicals infiltrating the cell wall and partially filling the lumen, (A4) chemicals only filling the lumen, and (A5) chemicals infiltrating the cell wall and filling the lumen. The unmodified molecular model includes vertical lines representing lignocellulosic polymers, empty circles representing hydroxyl groups, dashed lines representing hydrogen bonds, and solid lines representing covalent bonds. In the modified molecular models, increasing distance between lignocellulosic polymers indicates swelling, and small filled circles represent hydroxyl groups that chemically reacted with the infiltrated chemical to form a covalent bond. Modified molecular scale models include (B2) bulking with cross-linking with wood polymers, (B3) bulking with covalent bonding of chemical to lignocellulosic chain, (B4) bulking without covalent bonding, and (B5) bulking with the creation of an interpenetrating polymer network (IPN)

changes in E_s^{NI} or H caused by treatments. A few lumina in the Si XFM maps of Figs. 5, 6 and 7 were also observed to be partially or fully filled by organosilicons. The inhomogeneity in the Si large-view XFM maps in Fig. 3 also suggested that some lumina, especially in the earlywood, were being filled by organosilicons. The higher WPG_{BW} values than WPG_{CW} values also supported organosilicons deposited in lumina. Collectively, these observations indicate that the cells in the treated wood can be classified as a mixture of cell wall models A2, A3, and A5 with infiltrated cell walls and different amounts of lumen filling. These results are the same as we reported for these organosilicon treatments for archeological oak wood (Broda et al. 2023).

The amount of infiltration into the cell wall may play a role in the effectiveness of organosilicon treatments. For instance, Papadopoulos and Hill found that for a series of different sized linear chain carboxylic acid anhydrides, the effect on moisture uptake and the resulting wood swelling arises more from the volume of chemicals embedded in the cell wall than from the reduction in the number of hydroxyl groups due to chemical modification (Papadopoulos and Hill 2003). Therefore, the effectiveness of a treatment to prevent shrinkage in moderately degraded waterlogged archaeological wood may also be approximately

proportional to the amount of chemicals infiltrated into the cell wall. The results of our previous study on the stabilization of waterlogged archeological oak wood by organosilicons followed this proportionality approximation in which the magnitude of WPG_{CW} correlated with the decrease in wood shrinkage caused by MTMS, MPTMS, or DEAPTMDS treatments (Broda et al. 2023). In the present study, the WPG_{CW} for MPTMS-treated samples (Table 3) was similar to the reduction in wood shrinkage, which agrees with previous research. However, a considerable difference can be observed for BP treated with MTMS and ChP treated with MTMS and DEAPTMDS. In these treatments, the reduction in shrinkage values was 9–12 percentage points higher than that expected on the basis of WPG_{CW}, which could suggest that the treatments were more effective than anticipated based on the WPG_{CW} measurements. Interestingly, although MTMS was effective in stabilizing BP (ASE of about 79%), even though MTMS-treated ChP had a higher than anticipated reduction in shrinkage based on $WPG_{CW,}$ it was still ineffective with an ASE_V of only about 52%. A comparison between WPG_{CW} and reduction in wood shrinkage could not be made for DEAPTMDS-treated BP because the µXFM experiments were impossible. Nevertheless, for both BP and ChP, the DEAPTMDS treatment is considered effective in stabilizing the degraded wood with an ASE_V of 74–75%.

Differences in molecular modifications may help to explain why different organosilicon treatments had different effects on wood. While DEAPTMDS is expected to be model B4 because it cannot polymerize nor create covalent bonds with wood polymers (Popescu and Broda 2021), the molecular modification models for MTMS and MPTMS are uncertain. Both MTMS and MPTMS could be models B2 or B3 if they react with wood polymers (and we know that this is possible (Popescu and Broda 2021)), model B5 if they self-polymerize inside the cell wall to create an interpolymer network (IPN) (which is possible, too), or model B4 if they do not self-polymerize or react with wood polymers.

One possible reason why MTMS was more effective when applied to BP than ChP is that it may have created an IPN (model B5) that reinforced and more effectively prevented shrinkage than the unreacted monomers by themselves (model B4) or the monomers covalently bonded to wood polymers (models B2 or B3). The potential formation of an IPN would likely depend on the number of monomers in the cell wall, as can be estimated from Nm in Table 3. The MTMS-treated BP had an Nm value of 0.9 mmol per cm^{-3}. The 0.9 nmol per cm^{-3} value for MTMS-treated BP is among the highest measured in this study, and in our previous study using archaeological oak (Broda et al. 2023). Some additional insights into the potential formation of an IPN can be gained from the nanoindentation results because an IPN would be expected to increase the cell wall mechanical properties, as observed in a previous study about how different isocyanates reacted within wood cell walls (Jakes et al. 2010). However, our nanoindentation results did not show an increase in mechanical properties (Table 4). The cell wall mechanical properties of MTMS-treated BP were observed to decrease compared to BPc, which does not directly support the formation of an IPN.

The surprisingly low amount of MTMS in ChP wood compared to BP apparently results from the different chemical compositions and structures of ChP and

BP. As seen from Table 1, besides the degree of degradation, the biggest differences between ChP and BP are in the number of free hydroxyls available (about 40% higher for ChP than BP), in bulk density of dry wood (about half-again higher for ChP), and in the equilibrium moisture content (over one third higher for ChP). Both BP and ChP have similar measured total pore volume and surface area in their cell walls. There were also differences in the cell wall chemistry of the studied wood. In BP, partial degradation of hemicelluloses, celluloses, and also lignin modification was observed along with the reduction in cellulose crystallinity, while in ChP, mainly hemicelluloses and lignin were degraded, with a concurrent decrease in cellulose crystallinity and the formation of cellulose II due to the alkaline treatment (Broda et al. 2022a). Additionally, as seen in Fig. 7a–d, the cell walls of ChP were pushed into the lumina creating smaller misshapen lumina, which may indicate structural damage in the cell walls caused by the NaOH degradation. The lumina may have been misshapen as the cell walls shrank during drying or by swelling forces during treatment. The possible swelling forces during treatment may have at least in part arisen from the increased spacing of the cellulose lattice caused by NaOH treatment (Nishiyama et al. 2000; Cai et al. 2015; Raia et al. 2021). It seems that structural and chemical differences between the analyzed wood types may affect the interactions with organosilicon compounds, as well as the kind of organosilicon applied. Perhaps the presence of Na ions remaining after the chemical degradation process inside the ChP cell walls also plays a role in the process, somehow blocking access to organosilicon molecules.

The differences in the wood chemical composition, structure, and other properties due to applied degradation techniques affect the effectiveness of the treatment, showing that the conservation method should be tailored to the needs of an individual object. Some aspects of how the different organosilicon treatments translated into dimensional stability of wood degraded differently remain unclear. The uncertainty of how MTMS and MPTMS modify wood at the molecular scale is one of the largest contributors to this uncertainty. Differences in cell wall molecular- and nanostructures in the different wood types also likely contributed to the differences. Therefore, future studies of how the degradation modifies the wood cell wall and how organosilicons chemically react or interact with wood polymers within a wood cell wall are needed. Another difficulty in comparing the cell wall μXFM and nanoindentation results to the bulk wood dimensional stability results is that the cell wall measurements were only done in latewood. Differences between earlywood and latewood may obscure the results, especially if degradation differs between earlywood and latewood. Future work should also examine the differences between earlywood and latewood.

Conclusion

The present research aimed at determining the mechanism of wood stabilization by organosilicons intended for the conservation of waterlogged archaeological wood. Experiments were performed on model chemically degraded and biologically degraded Scots pine, which differed in the degree of degradation,

structure, and chemical composition. The three organosilicons studied included the two silanes MTMS and (MPTMS, as well as the siloxane DEAPTMDS. The large-field view XFM results revealed that all applied organosilicons penetrated throughout the whole wooden blocks during treatment. The collective bulk wood, multiscale XFM, and nanoindentation results revealed that the organosilicon treatments in this study can be classified as a mixture of Norimoto cell wall modification models A2, A3, and A5 with organosilicons infiltrating the cell walls and partially or entirely filled the cell lumina. For a given treatment, more organosilicon infiltrated in BP than ChP, likely because BP wood cell walls had a higher measured total pore volume and surface area. Based on ASE_v, all treated model degraded wood had acceptable values between 74 and 82%, except for MTMS-treated ChP, with a substantially lower ASE_V value of about 52%. The MTMS-treated ChP had the lowest measured latewood WPG_{CW}. It remains unclear why the MTMS did not infiltrate the ChP latewood cell walls. However, the low WPG_{CW} likely caused the low ASE_V value, which further supports that cell wall infiltration is an important mechanism for organosilicons to act as effective consolidants for waterlogged archaeological wood.

Degradation processes had a modest effect on the E_s^{NI} and H of ChP and BP cell walls despite their high mass losses. These modest effects support that after wood polymers are removed from the cell wall during degradation, upon drying the wood polymers coalesce and fill in the volumes vacated by the removed polymers to reform a solid material. For all wood types, DEAPTMDS treatments decreased E_s^{NI} and H, which resulted from a plasticization effect. Concerning Norimoto molecular wood modification models, DEAPTMDS treatment fits model B4 because it penetrates the cell wall, cannot polymerize, and does not react with wood polymers. A hydrophilic molecule like DEAPTMDS with a model B4 molecular model may have a plasticizing effect on the cell wall, as observed here. The DEAPTMDS plasticizing effect was much stronger in ChP and BP than in CP, which clearly indicated that the wood polymers in the latewood S2 cell wall layer were degraded. The effects of alkoxysilane (MTMS and MPTMS) treatments on cell wall mechanical properties were more modest and depended on the wood type and treatment type. The different effects of alkoxysilanes likely arose because of different potential molecular scale interactions that could occur when they infiltrated the cell walls. Because MTMS and MPTMS can react with wood polymers and also self-polymerize inside the cell wall to create an interpenetrating polymer network, potential Norimoto molecular models B2, B3, or B5 are possible. Further chemical analyses that can better discern which molecular interactions are occurring with the wood polymers would be beneficial for identifying the stabilization mechanism and understanding the differences between MTMS and MPTMS treatments.

Considering the above information, although DEAPTMDS was very effective in stabilizing waterlogged wood dimensions, the fact that it was in a liquid state inside the wood structure when applied on biologically degraded pine, making the samples wet and sticky, excludes it from the conservation practice before recognizing the reason behind this behavior. MTMS and MPTMS seem more promising conservation agents, but broader knowledge about their long-term behavior is needed before recommending them for practical application.

Based on the results obtained, it can be stated that the final effect of organosilicon treatment on the dimensional wood stabilization and mechanical properties of wood cell walls is not universal and depends on the degree and type of wood degradation (and the resulting differences in their chemical composition, structure and other properties), the applied organosilicon, the organosilicon's retention in wood, and the degree of polymerization and reactivity with wood polymers. Therefore, to tailor the conservation treatments to the needs of individual wooden objects, more research is needed to understand better the complex interactions between organosilicons and wood.

Author contributions MB and JEJ wrote the main manuscript text; JEJ prepared Figs. 2, 3, 4, 5, 6, 7 and 8; MB prepared Tables 1, 2, 3 and 4, Fig. 1 and contributed to Fig.2; LL, OAA, ERM and QJ conducted XFM analyses; MB prepared wood samples; MB and JEJ conducted nanoindentation. All authors reviewed the manuscript.

Funding This research was partially supported by the Polish–U.S. Fulbright Commission through a Fulbright Senior Award 2020/21 granted to Magdalena Broda and funded by the USDA Forest Products Laboratory, Madison, WI, US. Wood impregnation with organosilicon compounds was supported by the Polish Ministry of Science and Higher Education within the "Cultural heritage—research into innovative solutions and methods for historic wood conservation" project (No. 2bH 15 0037 83). This research used resources from the Advanced Photon Source, a US Department of Energy (DOE) Office of Science User Facility operated for the DOE Office of Science by Argonne National Laboratory under Contract No. DE-AC02-06CH11357. The work by Qiaoling Jin was supported by NIH Biotechnology Resources Grants P41, project number 1P41GM135018-01, project title: Quantitative Elemental Mapping for the Life Sciences, PI: O'Halloran, Thomas V. (Department of Chemistry, Michigan State University, East Lansing, MI 48824) Jacobsen, Chris Johnson (XSD, Argonne). This research was supported in part by the U.S. Department of Agriculture, Forest Service.

Declarations

Conflict of interest On behalf of all authors, the corresponding author states that there is no conflict of interest.

References

Bengtsson M, Oksman K (2006) The use of silane technology in crosslinking polyethylene/wood flour composites. Compos A Appl Sci Manuf 37:752–765. https://doi.org/10.1016/j.compositesa.2005.06.014

Broda M, Plaza NZ (2023) Durability of model degraded wood treated with organosilicon compounds against fungal decay. Int Biodeter Biodegr 178:105562. https://doi.org/10.1016/j.ibiod.2022.105562

Broda M, Yelle DJ (2022) Reactivity of waterlogged archeological elm wood with organosilicon compounds applied as wood consolidants: 2D 1H–13C solution-state NMR studies. Molecules 27:3407. https://doi.org/10.3390/molecules27113407

Broda M, Majka J, Olek W, Mazela B (2018a) Dimensional stability and hygroscopic properties of waterlogged archaeological wood treated with alkoxysilanes. Int Biodeter Biodegr 133:34–41. https://doi.org/10.1016/j.ibiod.2018.06.007

Broda M, Mazela B, Frankowski M (2018b) Durability of wood treated with aatmos and caffeine-towards the long-term carbon storage. Maderas Ciencia y Tecnología 20:455–468. https://doi.org/10.4067/S0718-221X2018005031501

Broda M, Mazela B, Dutkiewicz A (2019a) Organosilicon compounds with various active groups as consolidants for the preservation of waterlogged archaeological wood. J Cult Herit 35:123–128. https://doi.org/10.1016/j.culher.2018.06.006

Broda M, Mazela B, Radka K (2019b) Methyltrimethoxysilane as a stabilising agent for archaeological waterlogged wood differing in the degree of degradation. J Cult Herit 35:129–139. https://doi.org/10.1016/j.culher.2018.06.004

Broda M, Dąbek I, Dutkiewicz A et al (2020) Organosilicons of different molecular size and chemical structure as consolidants for waterlogged archaeological wood–a new reversible and retreatable method. Sci Rep 10:1–13. https://doi.org/10.1038/s41598-020-59240-8

Broda M, Spear MJ, Curling SF, Ormondroyd GA (2021) The viscoelastic behaviour of waterlogged archaeological wood treated with methyltrimethoxysilane. Materials 14:5150. https://doi.org/10.3390/ma14185150

Broda M, Popescu CM, Curling SF et al (2022a) Effects of biological and chemical degradation on the properties of scots pine wood—part I: chemical composition and microstructure of the cell wall. Materials 15:2348. https://doi.org/10.3390/ma15072348

Broda M, Spear MJ, Curling SF, Dimitriou A (2022b) Effects of biological and chemical degradation on the properties of scots pine—part II: wood-moisture relations and viscoelastic behaviour. Forests 13:1390. https://doi.org/10.3390/f13091390

Broda M, Jakes JE, Li L, Antipova OA (2023) Archeological wood conservation with selected organosilicon compounds studied by XFM and nanoindentation. Wood Sci Technol 57:1277–1298. https://doi.org/10.1007/s00226-023-01503-4

Cai M, Takagi H, Nakagaito AN et al (2015) Influence of alkali treatment on internal microstructure and tensile properties of abaca fibers. Ind Crops Prod 65:27–35. https://doi.org/10.1016/j.indcrop.2014.11.048

Donath S, Militz H, Mai C (2004) Wood modification with alkoxysilanes. Wood Sci Technol 38:555–566. https://doi.org/10.1007/s00226-004-0257-1

Donath S, Militz H, Mai C (2006) Treatment of wood with aminofunctional silanes for protection against wood destroying fungi. Holzforschung 60:210–216. https://doi.org/10.1515/HF.2006.035

Giudice CA, Alfieri PV, Canosa G (2013) Decay resistance and dimensional stability of Araucaria angustifolia using siloxanes synthesized by sol–gel process. Int Biodeterior Biodegrad 83:166–170. https://doi.org/10.1016/j.ibiod.2013.05.015

Glass S, Zelinka S (2021) Moisture relations and physical properties of wood. Chapter 4 in general technical report FPL-GTR-282 4–22

Glowacki AT, and USDOE. XRF-MAPS. Computer software. https://www.osti.gov//servlets/purl/1814636. USDOE. 3 Oct. 2020. Web. https://doi.org/10.11578/dc.20210824.5

Grattan DW (1987) Waterlogged wood. Conservation of marine archaeological objects. Elsevier, pp 55–67

Hayeemasae N, Adair A, Soontaranon S et al (2023) Optimising silane coupling agent content in phenolic-resin-cured sepiolite-filled natural rubber composites. J Rubber Res. https://doi.org/10.1007/s42464-023-00210-w

Henke BL, Gullikson EM, Davis JC (1993) X-ray interactions: photoabsorption, scattering, transmission, and reflection at E = 50–30,000 eV, Z = 1–92. At Data Nucl Data Tables 54:181–342. https://doi.org/10.1006/adnd.1993.1013

Hill CA, Farahani MM, Hale MD (2004) The use of organo alkoxysilane coupling agents for wood preservation. Holzforschung 58(3):316–325. https://doi.org/10.1515/HF.2004.049

Jakes JE, Stone DS (2021) Best practices for quasistatic berkovich nanoindentation of wood cell walls. Forests 12:1696. https://doi.org/10.3390/f12121696

Jakes JE, Yelle DY, Beecher JF, et al (2010) Characterizing polymeric methylene diphenyl diisocyanate reactions with wood: 2. Nano-indentation. In: Proceedings of International Conference on Wood Adhesives. Lake Tahoe, Nevada, USA, September 28-30, 2009, pp 366–373

Jakes JE, Hunt CG, Yelle DJ et al (2015) Synchrotron-based X-ray fluorescence microscopy in conjunction with nanoindentation to study molecular-scale interactions of phenol-formaldehyde in wood cell walls. ACS Appl Mater Interfaces 7:6584–6589. https://doi.org/10.1021/am5087598

Jakes JE, Frihart CR, Hunt CG et al (2019) X-ray methods to observe and quantify adhesive penetration into wood. J Mater Sci 54:705–718. https://doi.org/10.1007/s10853-018-2783-5

Jakes JE, Zelinka SL, Hunt CG et al (2020) Measurement of moisture-dependent ion diffusion constants in wood cell wall layers using time-lapse micro X-ray fluorescence microscopy. Sci Rep 10:9919. https://doi.org/10.1038/s41598-020-66916-8

Kennedy A, Pennington ER (2014) Conservation of chemically degraded waterlogged wood with sugars. Stud Conserv 59:194–201. https://doi.org/10.1179/2047058413Y.0000000109

Kirker G, Zelinka S, Gleber S-C et al (2017) Synchrotron-based X-ray fluorescence microscopy enables multiscale spatial visualization of ions involved in fungal lignocellulose deconstruction. Sci Rep 7:41798. https://doi.org/10.1038/srep41798

Kumar A, Ryparová P, Škapin AS et al (2016) Influence of surface modification of wood with octadecyltrichlorosilane on its dimensional stability and resistance against Coniophora puteana and molds. Cellulose 23:3249–3263. https://doi.org/10.1007/s10570-016-1009-8

Liu L, Zhang L, Zhang B, Hu Y (2019) A comparative study of reinforcement materials for waterlogged wood relics in laboratory. J Cult Herit 36:94–102. https://doi.org/10.1016/j.culher.2018.08.002

Mai C, Militz H (2004) Modification of wood with silicon compounds. Inorganic silicon compounds and sol-gel systems: a review. Wood Sci Technol 37:339–348. https://doi.org/10.1007/s00226-003-0205-5

Marciniec B (2009) Hydrosilylation: a comprehensive review on recent advances. Advances in silicon science. Springer, Dordrecht

Nishiyama Y, Kuga S, Okano T (2000) Mechanism of mercerization revealed by X-ray diffraction. J Wood Sci 46:452–457. https://doi.org/10.1007/BF00765803

Norimoto M (2001) Chemical modification of wood. In: Hon DN-S, Shirashi N (eds) Wood and cellulose chemistry, 2nd edn. Marcel Dekker, New York, pp 573–598

Panov D, Terziev N (2009) Study on some alkoxysilanes used for hydrophobation and protection of wood against decay. Int Biodeter Biodegr 63:456–461. https://doi.org/10.1016/j.ibiod.2008.12.003

Papadopoulos AN, Hill CAS (2003) The sorption of water vapour by anhydride modified softwood. Wood Sci Technol 37:221–231. https://doi.org/10.1007/s00226-003-0192-6

Paunesku T, Vogt S, Maser J et al (2006) X-ray fluorescence microprobe imaging in biology and medicine. J Cell Biochem 99:1489–1502. https://doi.org/10.1002/jcb.21047

Popescu C-M, Broda M (2021) Interactions between different organosilicons and archaeological waterlogged wood evaluated by infrared spectroscopy. Forests 12:268. https://doi.org/10.3390/f12030268

Raia RZ, Iwakiri S, Trianoski R et al (2021) Effects of alkali treatment on modification of the *Pinus* fibers. Matéria (rio j) 26:e12936. https://doi.org/10.1590/S1517-707620210001.1236

Sae-oui P, Sirisinha C, Thepsuwan U, Hatthapanit K (2006) Roles of silane coupling agents on properties of silica-filled polychloroprene. Eur Polymer J 42:479–486. https://doi.org/10.1016/j.eurpolymj.2005.09.003

Salmén L, Burgert I (2009) Cell wall features with regard to mechanical performance. A review COST Action E35 2004–2008: wood machining – micromechanics and fracture. Holzforschung 63:121–129. https://doi.org/10.1515/HF.2009.011

Schindelin J, Arganda-Carreras I, Frise E et al (2012) Fiji: an open-source platform for biological-image analysis. Nat Methods 9:676–682. https://doi.org/10.1038/nmeth.2019

Schorr D, Blanchet P (2020) Improvement of white spruce wood dimensional stability by organosilanes sol-gel impregnation and heat treatment. Materials 13:973. https://doi.org/10.3390/ma13040973

Sèbe G, Tingaut P, Safou-Tchiama R et al (2004) Chemical reaction of maritime pine sapwood (Pinus pinaster Soland) with alkoxysilane molecules: a study of chemical pathways. Holzforschung 58:511–518. https://doi.org/10.1515/HF.2004.078

Tahira A, Howard W, Pennington ER, Kennedy A (2017) Mechanical strength studies on degraded waterlogged wood treated with sugars. Stud Conserv 62:223–228. https://doi.org/10.1080/00393630.2016.1169364

Tang W, Jian Y, Shao M et al (2023) A novel two-step strategy to construct multifunctional superhydrophobic wood by liquid-vapor phase deposition of methyltrimethoxysilane for improving moisture resistance, anti-corrosion and mechanical strength. Colloids Surf, A 666:131314. https://doi.org/10.1016/j.colsurfa.2023.131314

Tshabalala MA, Kingshott P, VanLandingham MR, Plackett D (2003) Surface chemistry and moisture sorption properties of wood coated with multifunctional alkoxysilanes by sol-gel process. J Appl Polym Sci 88:2828–2841. https://doi.org/10.1002/app.12142

Vogt S (2003) MAPS : a set of software tools for analysis and visualization of 3D X-ray fluorescence data sets. J Phys IV France 104:635–638. https://doi.org/10.1051/jp4:20030160

Wang M, Bonfield W (2001) Chemically coupled hydroxyapatite–polyethylene composites: structure and properties. Biomaterials 22:1311–1320. https://doi.org/10.1016/S0142-9612(00)00283-0

Wimmer R, Lucas BN, Oliver WC, Tsui TY (1997) Longitudinal hardness and Young's modulus of spruce tracheid secondary walls using nanoindentation technique. Wood SciTechnol 31:131–141. https://doi.org/10.1007/BF00705928

Xie Y, Hill CA, Xiao Z et al (2010) Silane coupling agents used for natural fiber/polymer composites: a review. Compos Part A Appl Sci Manuf 41:806–819. https://doi.org/10.1016/j.compositesa.2010.03.005

Yona AMC, Žigon J, Matjaž P, Petrič M (2021) Potentials of silicate-based formulations for wood protection and improvement of mechanical properties: a review. Wood Sci Technol 55:887–918. https://doi.org/10.1007/s00226-021-01290-w

Yu Y, Fei B, Wang H, Tian G (2011) Longitudinal mechanical properties of cell wall of Masson pine (Pinus massoniana Lamb) as related to moisture content: a nanoindentation study. Holzforschung 65:121–126. https://doi.org/10.1515/hf.2011.014

Zelinka SL, Jakes JE, Tang J et al (2019) Fungal–copper interactions in wood examined with large field of view synchrotron-based X-ray fluorescence microscopy. Wood Mat Sci Eng 14:174–184. https://doi.org/10.1080/17480272.2018.1458049

Authors and Affiliations

Magdalena Broda[1] · Joseph E. Jakes[2] · Luxi Li[3] · Olga A. Antipova[3] · Evan R. Maxey[3] · Qiaoling Jin[4]

✉ Magdalena Broda
magdalena.broda@up.poznan.pl

✉ Joseph E. Jakes
joseph.e.jakes@usda.gov

[1] Department of Wood Science and Thermal Techniques, Faculty of Forestry and Wood Technology, Poznan University of Life Sciences, Wojska Polskiego 38/42, 60-637 Poznan, Poland

[2] Forest Products Laboratory, Forest Biopolymers Science and Engineering, USDA Forest Service, One Gifford Pinchot Drive, Madison, WI 53726, USA

[3] X-Ray Science Division, Advanced Photon Source, Argonne National Laboratory, 9700 S. Cass Avenue, Lemont, IL 60439, USA

[4] Department of Physics and Astronomy, Northwestern University, 2145 Sheridan Road, Evanston, IL 60208, USA